

A CALIBRATED COMPUTER MODEL FOR THE THERMAL SIMULATION OF COURTYARD MICROCLIMATES

Amr Bagneid, and Jeffrey Haberl, Ph.D., P.E.
College of Architecture, Texas A&M University

ABSTRACT

This paper describes a calibrated stand-alone courtyard microclimate model. This model is considered to be the first calibrated computer program for the simulation of courtyard microclimates. In order to accomplish this a calibrated simplified thermal simulation model for predicting courtyard microclimates was created that is based on a Finite Difference (FD) simulation model of an RC thermal network of the courtyard.

The courtyard microclimate model was validated against field data from a case study courtyard house. The model allowed running parametric sensitivity studies on the courtyard thermal simulation factors. The model was then used to produce annual hourly courtyard microclimate weather file for use by the DOE-2 building thermal simulation program.

This courtyard microclimate model is also a part of a larger research project that aims to analyze the thermal performance of courtyard houses. The overall project measured a case study courtyard house in the winter and summer for the calibration of the simulated courtyard microclimate, and then used the simulated microclimate weather file in a DOE-2 simulation of the courtyard house to better predict the courtyard house thermal performance.

This paper will describe the method used in creating the courtyard model and present results of its application to the case study courtyard.

INTRODUCTION

This research was produced as part of an effort to revive the use of courtyard housing clusters in a modern context, which were traditionally known for their distinctive passive cooling performance (Bagneid, 1989). The goal is to provide an assessment of its passive cooling performance by creating a building simulation tool that includes a thermal model for the courtyard microclimate; thus introducing an improvement to the current generation of building

simulation software. The objective is to develop a methodology that simulates the courtyard microclimate, which has been tested with actual field data from a case study, indigenous courtyard house in Cairo, Egypt. The case study house was built around 1400 AD, having an area of about 5000 sq. ft. (i.e., comparable to the site of a single-family house) with heavy thermal mass. To accomplish this, a finite difference thermal network was created for simulating the case study courtyard microclimate. This model allowed running parametric sensitivity studies on the courtyard design factors.

THE CASE STUDY COURTYARD HOUSE

The “Zeynab Khatun” (Lady Zeynab) traditional courtyard house was selected among a set of the remaining original traditional courtyard houses (25 houses) (Revault, 1997) in old Cairo as a case study house for field thermal monitoring. The restored house includes some features that are common in traditional Cairene courtyard houses: high thermal mass, wooden lattice window shades, shutter-less windows, high ceilings, marble floors with wall cladding, and dome vents. In general, building materials are limestone, marble, and wood. The house has two secondary courtyards besides the main courtyard: the kitchen and the service courtyards. To better analyze the thermal performance of the house a Finite Difference (FD) model was developed to study the thermal features of the main courtyard. Figure 1 includes a plan and a section of the case study house, showing the placement of the monitoring sensors that were used to collect summer and winter temperature data. Of particular interest to the current paper are the sensors in the main courtyard and above rooftop.

FINITE DIFFERENCE (FD) SIMULATION MODEL

In general, the limitations of the most commonly used current thermal simulation software (i.e., DOE-2, BLAST) are that inter-zonal airflow are not usually simulated. The hand-made approach applied in

creating this Finite Difference (FD) simulation model facilitated the modeling as well as the sensitivities testing on ACH rates.

Finite Difference (FD) models are widely used to analyze transient heat transfer problems. The FD method applied here uses an explicit solution scheme where the temperature of any node at a new time $t+1$ is calculated from the temperature at the same node and neighboring nodes for the previous time t . Figure 2 is a schematic diagram of the Finite Difference (FD) equivalent thermal circuit for the case study courtyard house. In this model, the house was represented using two lumped wall nodes representing the north and south thermal mass, with air nodes in between the walls. The courtyard house being approximately square shaped oriented 25 degrees east of north allowed to easily divide the house into a north zone composed of its north west and north east wings and a south zone composed of its south east and south west wings. The north wall nodes represent the NE & NW wings of the house while the south wall nodes represent the SE & SW wings of the courtyard house up to the height of the main courtyard (i.e., two floors). The mass and the width of each of the north and south wall nodes were calculated respectively with the consideration of dividing the case study courtyard house into two zones: north and south. The nominal face area of the wall nodes represents the equivalent area of the walls in the main courtyard.

In the FD model, the equivalent courtyard model was divided into two zones: lower and upper, that corresponds to the temperature measurements taken on site. Each section contains, at its center, an air node for the thermal heat balance. Each air node has natural convection with the ambient air: the upper node communicates with the above courtyard ambient air node, and the lower node communicates with the street ambient air node (through the house entry gate). Also the upper and lower nodes communicate with each other. Each air node in the lower or upper courtyard sections also have convection exchange with the other nodes on the courtyard envelope as shown on Figure 2.

The FD model used one-dimensional, lumped thermal mass walls to simplify the analyses. All the internal nodes have material of width ($\Delta x/4$) associated with them on either side of their center plane, and the boundary nodes have material of width ($\Delta x/4$). The temperature balance at the surface nodes considers solar radiation, natural convection, conduction, and sky radiation. Direct and diffuse solar radiation were obtained through modeling the courtyard in DOE-2 and producing the hourly values for each of the courtyard envelope surfaces. Radiation between the courtyard envelope surfaces was assumed to be small compared

to the convection and conduction components, hence it was ignored. The temperatures for the nodes inside the wall or in the ground were calculated using conduction only. The temperatures for the ambient air and the ground were assigned from climatic records. The simulated air temperature for the two nodes inside the courtyard (upper and lower) were compared to field measurements in order to calibrate the model. Table 1 includes a list of the heat balance equations for each node along with their stability criterion. The equations were developed through an energy balance and they were checked manually. Boundary checks were performed, and convergence as well as sensitivity runs were made.

To verify the model convergence, tests were used to determine the time it takes to reach steady state condition. In these tests synthetic weather data was used to determine the convergence time. The tests showed that the model reached convergence in a minimum of about 11-1/2 months.

CALIBRATION OF THE FD MODEL

Measured hourly courtyard microclimate temperatures at two heights ($T_{c1}= 10\text{ft.}$ and $T_{c2}= 20\text{ft.}$) were used to see how well the model predicted the actual performance of the courtyard for two 21 days periods in August, 2001, and in December 2001 to January 2002. Once the simulated temperatures matched the measured data in a satisfactory way, the FD microclimate model was then used to predict annual conditions in the courtyard, which were driven by measured weather data from a nearby weather station.

To determine how well the FD model simulated the actual conditions in the case study courtyard house, several statistical analyses were used including, the Coefficient of Variation for the Root Mean Squared Error ((CV)RMSE) and the Normalized Mean Biased Error (NMBE) (Kreider and Haberl, 1994). The criteria established by ASHRAE Guideline 14 (2002), which sets uncertainty or tolerance limits for calibrated simulation of NMBEs within $\pm 10\%$, and (CV)RMSEs within $\pm 30\%$ (hourly data), were considered. The FD thermal network model showed high levels of performance during its calibration process. In this analysis annual simulations were made using the courtyard FD thermal network model, and comparisons were made with the two periods of measured data. Parametric analyses were performed for a number of variables, including: air change rates, thermal mass, solar absorption, etc. Figure 3 shows an example of the parametric runs with the resulting microclimate $(T_{c1} + T_{c2})/2$ °F while applying different air change (ACH) rates.

In this analysis a daily schedule was applied to the courtyard ACH for the lower courtyard node since the entry gate to the house closes during the night. Two rates were applied to the ACH rates between the courtyard nodes and ambient air: the first, which is named ‘Type I’ has the ACH between the upper node (T_{c1}) and ambient air equal to (a 70% ACH), with the ACH between the courtyard lower node (T_{c2}) and ambient air equal to (a 30% ACH), and the second which is named ‘Type II’ having the ACH between the upper node and ambient air equal to (a 90% ACH) with the ACH between the courtyard lower node and ambient air equal to (a 10% ACH). In both types the ACH between the upper and lower nodes is 50% in both directions. Runs were then made while varying the courtyard ACH rates between 5, 20, 40, 60, 120, and 180. The airflow percentages between the nodes considered both type I & II simulations, making a total of 12 runs = 6ACH rates x 2 airflow percentages.

In all runs the total house mass plus all of the internal mass that gave the best results from the first calibration was applied. Figure 3 shows the second six runs for the six ACH rates with Type II airflow percentage between nodes. Among these twelve runs an estimated ACH of 35 (a point between 20 ACH & 40 ACH runs) for both Types I & II air change percentage showed the best (CV)RMSE & NMBE results considering summer and winter periods.

Figures 4 a&b shows a close-up of the hottest and coldest days of the year respectively for sensitivities runs where the courtyard walls and floors solar absorptivity values were varied (actual value (65%), actual value+20%, actual value-20%) to test their impact on the resulting courtyard microclimate temperatures. During the hottest days, the run with the absorptivity value increased by 20% (i.e., 85%) produced simulated temperatures that were similar to the base-case during the heating hours and hotter than the base-case during the cooling hours. During the hottest days, the run with the absorptivity value decreased by 20% (i.e., 45%) produced simulated temperatures that were less than the base-case during all the hours by <3F. During the coldest days, the simulations with the two new absorptivity values (i.e., 45% & 85%) showed a similar performance to the base-case (difference in simulated temperatures was less than 2F). Accordingly, the model may be labeled as significantly sensitive to absorptivity under the summer climate. During the winter this would not be valid, likely due to the existence of a cloud cover.

Figure 5 shows a full year run for the simulated courtyard microclimate dry-bulb temperature versus the rooftop dry-bulb temperature (measured during the

monitoring periods) combined with IWEC dry-bulb temperature.

CONCLUSION

A calibrated thermal simulation model for predicting courtyard microclimates was created that is based on a Finite Difference (FD) simulation model of an RC thermal network of the courtyard. The courtyard microclimate model was validated against field data from a case study courtyard house. This paper described the method used and presented results of its application to the case study courtyard. The results of the parametric analysis showed that the model was sensitive to variations in air change rates, solar absorptivity, and ambient air temperatures (Bagneid, 2006). It is believed that this model if applied to other courtyard shapes as well as climates would have a similar high level of simulation performance.

ACKNOWLEDGEMENTS

Portions of this work were supported by an American Society of Heating, Refrigerating, and Air-Conditioning Engineers (ASHRAE) Graduate Grant-In-Aid, as well as three American Institute of Architects and American Architectural Foundation (AIA/AAF) Fellowships for Advanced Research.

REFERENCES

- ASHRAE 14 (2002). Guideline 14-2002: Measurement of Energy and Demand Savings, American Society of Heating, Refrigerating and Air-Conditioning Engineers, Atlanta.
- Bagneid, A. (2006). The Creation of a Courtyard Microclimate Thermal Model for the Analysis of Courtyard Houses. Ph.D. Dissertation, Department of Architecture, Texas A&M University.
- Bagneid, A. (1989). Indigenous residential courtyards: typology, morphology, and bioclimates, International symposium: Traditional Dwellings and Settlements in a Comparative Perspective, Vol. 6: Courtyard as dwelling. (Pp.39-57), Berkeley: Center for Environmental Design Research, University of California.
- Kreider, J. and Haberl, J. 1994. "Predicting Hourly Building Energy Usage: The Results of the 1993 Great Energy Predictor Shootout Identify the Most Accurate Method for Making Hourly Energy Use Predictions", *ASHRAE Journal*, Volume 35, Number 3, pp. 72 - 81.
- Revault, Jacques, and Maury, Bernard (1979). "Palais et maisons du Caire" du XIV au XVIII Siecle". (Palaces and houses of Cairo form 14th to 18th century). Cairo: Institut Francaise d'Archeologie Orientale.

NOMENCLATURE

A	Surface Area (m^2) ($ft.^2$)
ACH	Air change per hour
Δt	Increment in time
Δx	Increment in distance
ASHRAE	American Society for Heating Refrigerating and Air-conditioning Engineers
Bi	Biot number
CLAC	Central Laboratory for Agricultural Climatology
C_p	Specific Heat ($2 \text{ kJ/kg} \cdot \text{K}$) ($\text{Btu}/(\text{lb}_m \cdot ^\circ\text{F})$)
F_o	Fourier number
FD	Finite Difference
h	Convection heat Transfer Coefficient ($\text{W}/m^2 \cdot \text{K}$) ($\text{Btu}/h \cdot \text{ft}^2$ $\cdot ^\circ\text{F}$)
IWEC	International Weather for Energy Calculations
K_{wall}	Thermal Conductivity ($\text{W}/m \cdot \text{K}$) ($\text{Btu}/h \cdot \text{ft} \cdot ^\circ\text{F}$)
k_T	Hourly Clearness Index
m	Mass airflow rate (lb/hr)
ρ	Density (kg/m^3) (lb_m/ft^3)
Q	Energy (Btu/hr)
T_{Tc}^{p+1}	Future node temperature at time p+1
T_{Tc}^p	Node temperature at time p

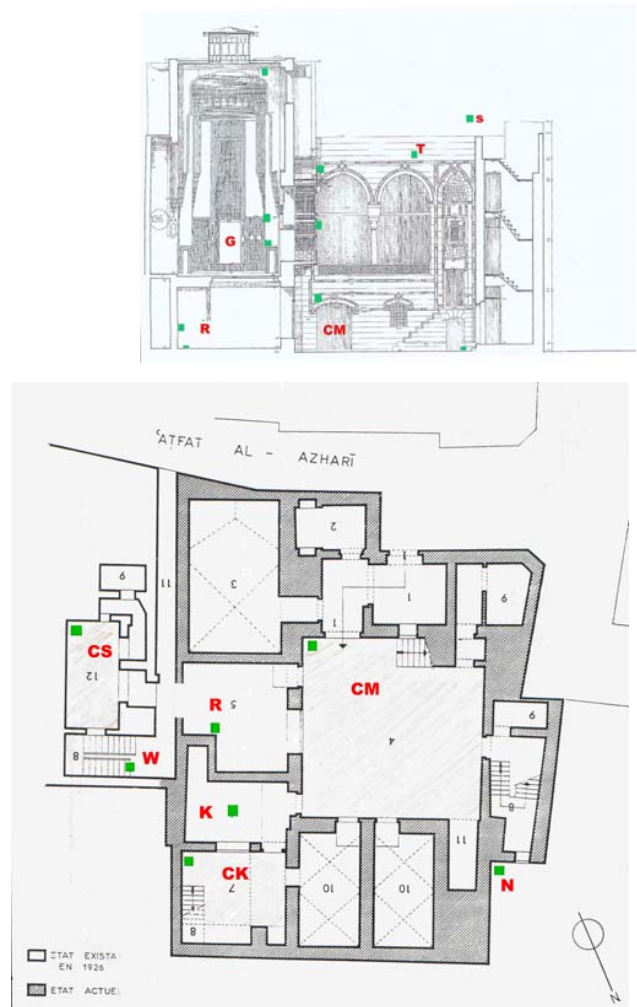


Figure 1 Ground Floor Plan & Section of the Case study House (Revault, 1997). Spaces: Main courtyard (CM), Service courtyard (CS), Kitchen courtyard (CK), Reception hall (R), summer hall (G), Rooftop solar Radiation shield (S). Note the places of the monitoring sensors in the main courtyard (CM), reception hall (R) & rooftop (S). Little square marks are the places of the sensors.

A I R	<p>Node T_{cl} $T_{cl}^p = (h_g A_g (T_{gi}^p) + h_{WIN} A_{WIN} (T_{WIN}^p) + h_{WIS} A_{WIS} (T_{WIS}^p) + m_{air(To-Tcl)} C_{p,air} (T_o^p) + m_{air(Tc2-Tcl)} C_{p,air} (T_{c2}^p)) / (h_{WIN} A_{WIN} + h_{WIS} A_{WIS} + h_g A_g + m_{air(To-Tcl)} C_{p,air} + m_{air(Tc2-Tcl)} C_{p,air})$</p> <p>Node T_{c2} $T_{c2}^p = (m_{air(Tcl-Tc2)} C_{p,air} (T_{cl}^p) + m_{air(To-Tc2)} C_{p,air} (T_o^p) + h_{W2N} A_{W2N} (T_{W2N}^p) + h_{W2S} A_{W2S} (T_{W2S}^p)) / (m_{air(Tcl-Tc2)} C_{p,air} + m_{air(To-Tc2)} C_{p,air} + h_{W2N} A_{W2N} + h_{W2S} A_{W2S})$</p>
W A L L S	<p>Node T_{WINi} # 1,4,9,12 $T_{WIN,i}^{p+1} = T_{WIN,i}^p (1 - 2Fo (B_i + 1)) + 2Fo T_{WIN,m}^p + 2B_i Fo T_{cl}^p + (Q_{solar} + Q_{sky,WIN}) / (\rho_{WIN} C_{p,WIN} \Delta_x)$</p> <p>Node T_{WIN,m} # 5,2,13,10 $T_{WIN,m}^{p+1} = T_{WIN,m}^p (1 - 2Fo) + Fo T_{WIN,i}^p + Fo T_{WIN,o}^p$</p> <p>Node T_{WIN,o} # 3,6,11,14 $T_{WIN,o}^{p+1} = T_{WIN,o}^p (1 - 2Fo (B_i + 1)) + 2Fo T_{WIN,m}^p + 2B_i Fo T_o^p$</p>
G R O U N D	<p>Node T_{Gi} # 7 $T_{G,i}^{p+1} = T_{G,i}^p (1.2Fo (B_i + 1)) + 2Fo T_{G,m}^p + 2B_i Fo T_{cl}^p + ((Q_{solar} + Q_{sky,G,i}) / (\rho_G C_{p,G} A_G \frac{\Delta_x}{2\Delta t}))$</p>
<p>Biot⁽²⁾ (B_i) and Fourier⁽³⁾ (Fo) numbers were used to simplify the expressions:</p>	
<p>$B_i = (h_{WIN} \Delta_x) / k_{avg}$ $Fo = \frac{K_{avg} \Delta t}{\rho_{WIN} C_{p,WIN} \Delta_x^2}$ $B_i Fo = \frac{h_{WIN} \Delta t}{\rho_{WIN} C_{p,WIN} \Delta_x}$</p>	
<p>1. To prevent unstable results τ must remain within the stability limit. To satisfy the stability criterion in a case of one-dimensional transient conduction, the value of τ should be determined as the minimum number among the calculated delta τ values for the nodes (or any time step less than this) which would satisfy the given conditions.</p> <p>2. The Biot number is a dimensionless measurement of the temperature change in the solid relative to the temperature difference between the surface and fluid.</p> <p>3. The Fourier number is a dimensionless time parameter that characterizes transient conduction heat transfer.</p>	
<p>STABILITY CRITERIA ⁽¹⁾</p> <p>$\Delta_t \leq \frac{\rho_{WIN} C_{p,WIN} \Delta_x^2}{2K_{avg} (B+1)}$</p> <p>$\Delta_t \leq \frac{\rho_{WIN} C_{p,WIN} \Delta_x^2}{2K_{avg}}$</p> <p>$\Delta_t \leq \frac{\rho_{WIN} C_{p,WIN} \Delta_x^2}{2K_{avg} (B+1)}$</p> <p>$\Delta_t \leq \frac{\rho_{WIN} C_{p,WIN} \Delta_x^2}{2K_{avg} (B+1)}$</p>	

Table 1 Finite Difference Model Equations

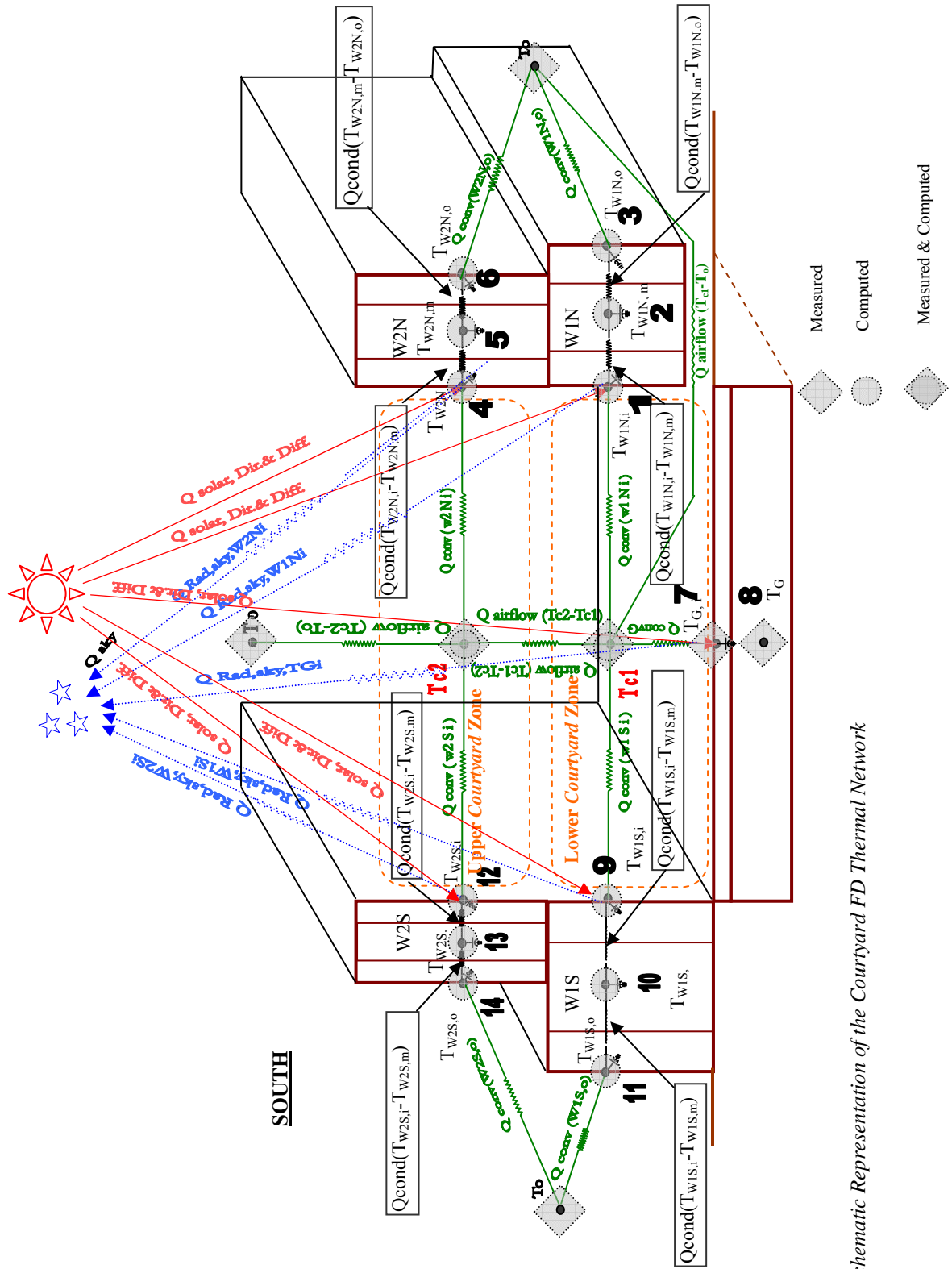


Figure 2 Schematic Representation of the Courtyard FD Thermal Network Model.

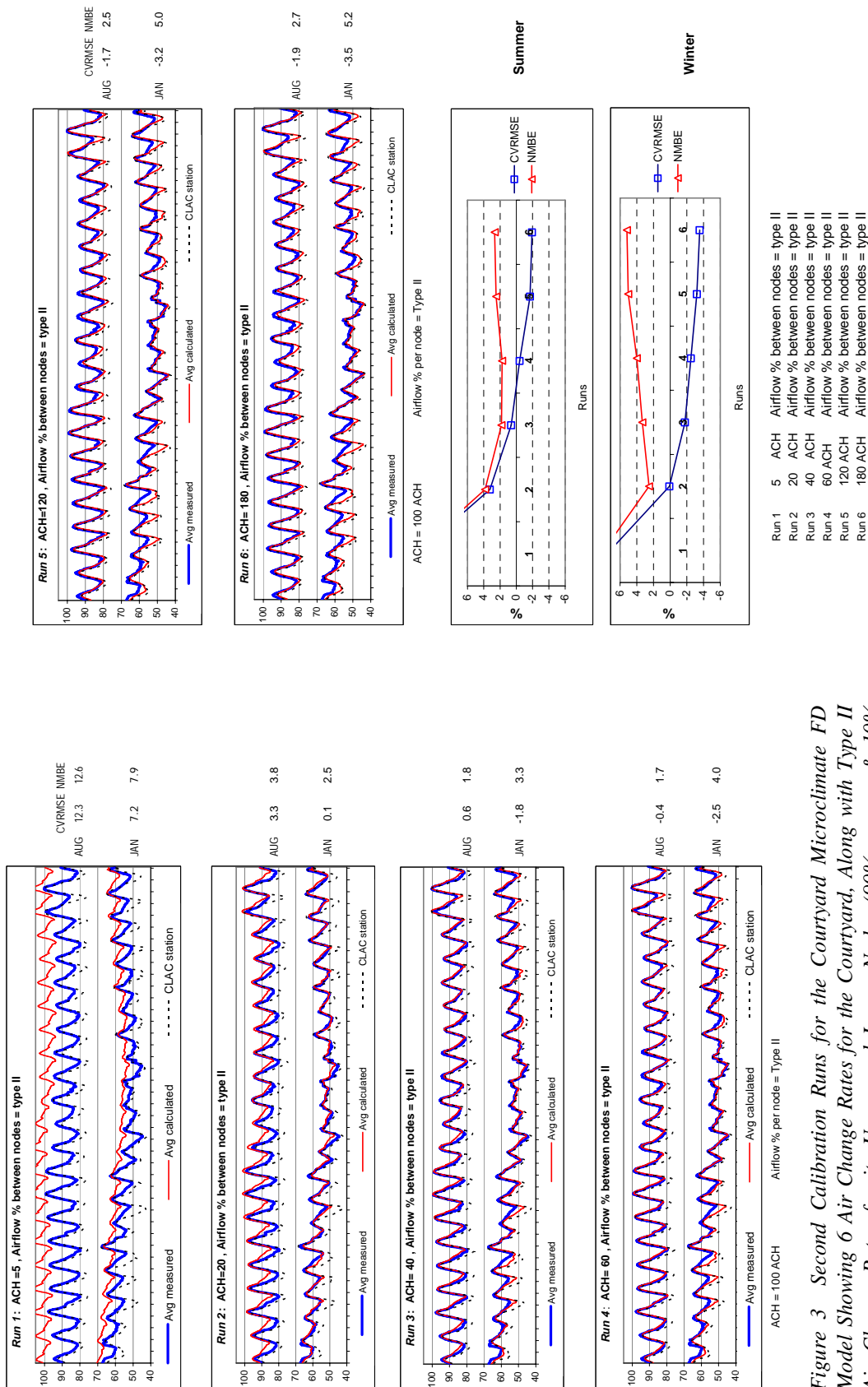


Figure 3 Second Calibration Runs for the Courtyard Microclimate FD Model Showing 6 Air Change Rates for the Courtyard, Along with Type II Air Change Rates for its Upper and Lower Nodes (90% upper & 10% lower).

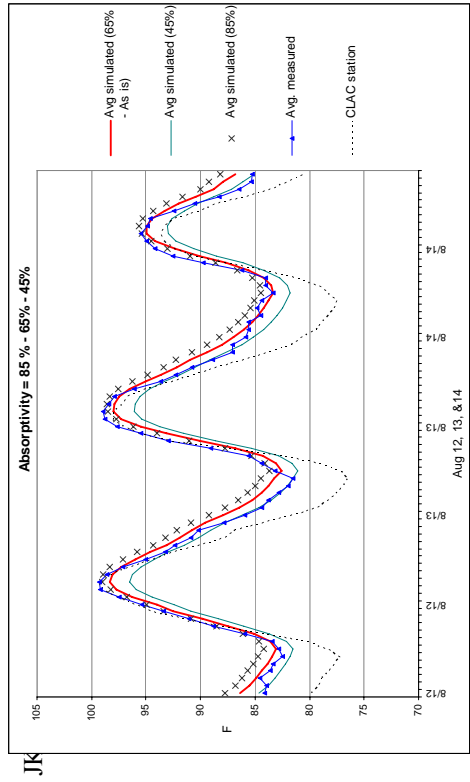


Figure 4a Sensitivity Runs for the Courtyard Microclimate FD model with Walls and Floor Solar Absorptivity Reduced 20% and Increased 20% of its Real Value. Close-up of the Three Hottest Summer Days.

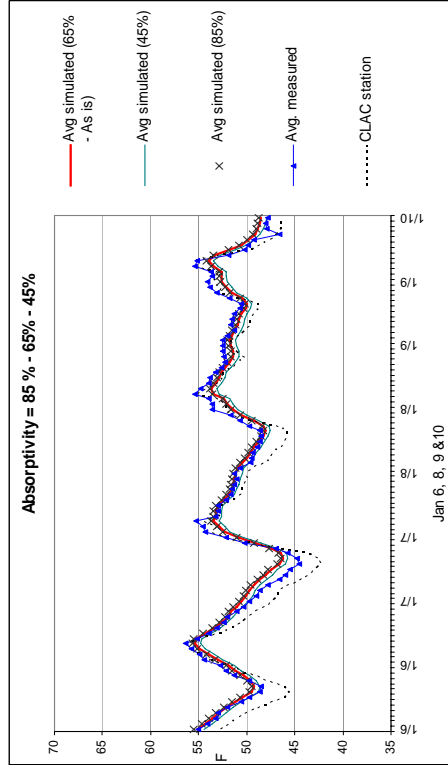


Figure 4b Sensitivity Runs for the Courtyard Microclimate FD Model with Walls and Floor Solar Absorptivity Reduced 20% and Increased 20% of its Real Value. Close-up of the Four Coldest Winter Days.

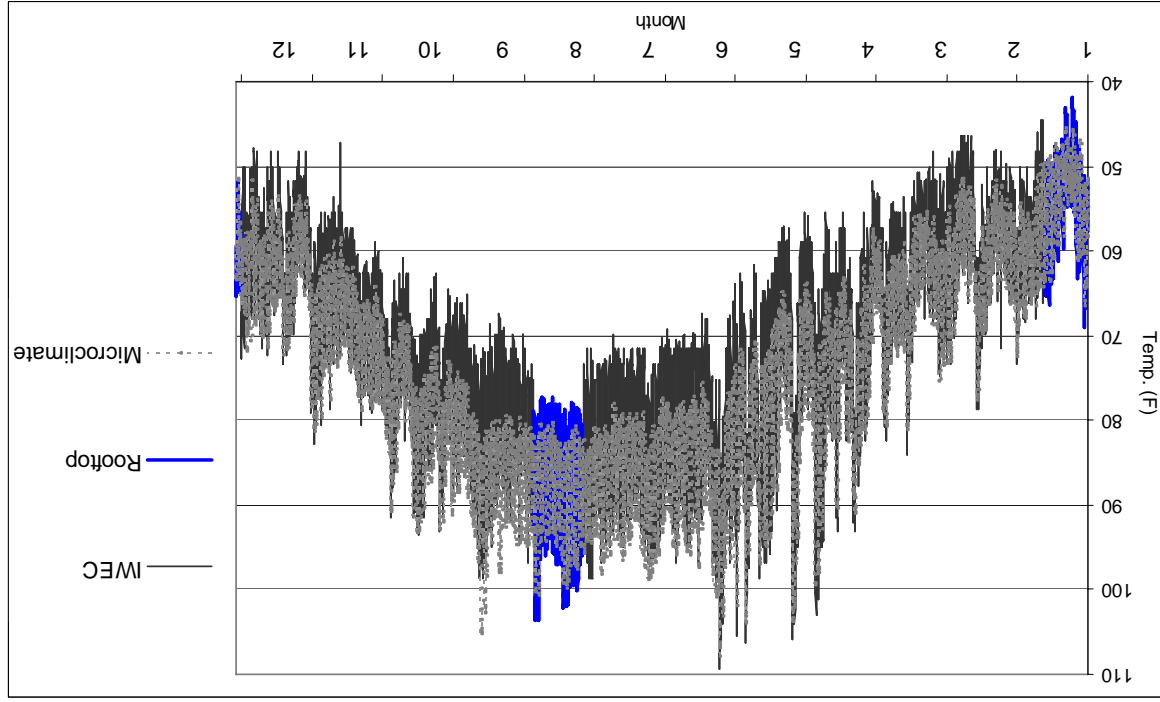


Figure 5 One Year of Hourly Simulated Courtyard Microclimate vs. the IWEC Weather File with Rooftop Temperature Records.